

Characteristics and possible causes of sea level anomalies in the Xisha sea area

WANG Hui¹, HAN Shuzong^{2*}, FAN Wenjing¹, WANG Guosong¹, LIU Kexiu¹, ZHANG Zengjian¹

¹ National Marine Data & Information Service, State Oceanic Administration, Tianjin 300171, China

² College of Oceanic and Atmospheric Sciences, Ocean University of China, Qingdao 266003, China

Received 16 October 2015; accepted 13 November 2015

©The Chinese Society of Oceanography and Springer-Verlag Berlin Heidelberg 2016

Abstract

Based on the analysis of wind, ocean currents, sea surface temperature (SST) and remote sensing satellite altimeter data, the characteristics and possible causes of sea level anomalies in the Xisha sea area are investigated. The main results are shown as follows: (1) Since 1993, the sea level in the Xisha sea area was obviously higher than normal in 1998, 2001, 2008, 2010 and 2013. Especially, the sea level in 1998 and 2010 was abnormally high, and the sea level in 2010 was 13.2 cm higher than the multi-year mean, which was the highest in the history. In 2010, the sea level in the Xisha sea area had risen 43 cm from June to August, with the strength twice the annual variation range. (2) The sea level in the Xisha sea area was not only affected by the tidal force of the celestial bodies, but also closely related to the quasi 2 a periodic oscillation of tropical western Pacific monsoon and ENSO events. (3) There was a significant negative correlation between sea level in the Xisha sea area and ENSO events. The high sea level anomaly all happened during the developing phase of La Niña. They also show significant negative correlations with Niño 4 and Niño 3.4 indices, and the lag correlation coefficients for 2 months and 3 months are -0.46 and -0.45, respectively. (4) During the early La Niña event from June to November in 2010, the anomalous wind field was cyclonic. A strong clockwise vortex was formed for the current in 25 m layer in the Xisha sea area, and the velocity of the current is close to the speed of the Kuroshio near the Luzon Strait. In normal years, there is a “cool eddy”. While in 2010, from July to August, the SST in the area was 2–3°C higher than that of the same period in the history.

Key words: Xisha sea area, sea level anomalies, ENSO, wind, current, SST

Citation: Wang Hui, Han Shuzong, Fan Wenjing, Wang Guosong, Liu Kexiu, Zhang Zengjian. 2016. Characteristics and possible causes of sea level anomalies in the Xisha sea area. *Acta Oceanologica Sinica*, 35(9): 34–41, doi: 10.1007/s13131-016-0938-2

1 Introduction

Under global warming, sea level rising and extreme ocean climate events have become a major global environmental problem. The 5th assessment report (AR5) of the Intergovernmental Panel on Climate Change (IPCC) noted that ocean thermal expansion and glacier mass loss are very likely the dominant contributors to global mean sea level rise during the 21st century. The rate of global mean sea level rise was 1.7 mm/a during 1901–2010 for a total sea level rise of 0.19 m. The rate was higher at 3.2 mm/a from 1993 to 2010. For the period of 2081–2100, compared to 1986–2005, global mean sea level rise is likely 0.26–0.82 m (IPCC, 2013). Sea level rise is the most significant in response to the global warming which has a large impact on humanity.

Regional sea level change and global averaged sea level change are significantly different. Regional sea level changes are affected not only by the global change, but also by the hydrological and meteorological factors such as local monsoon, ocean currents, SST, air pressure, precipitation and so on. The high or low sea level anomaly along the coastal region of China is caused by anomalous non-astronomical factors (including air pressure, wind, precipitation and runoff, etc.), leading to sea level short-term anomaly changes (Fang et al., 1986; Wang et al., 2012). In the coastal region of China, high sea level anomaly in a short

period is closely related to the changes of monsoon. It mainly operates through changes in residual water caused by the surface Ekman transport (including Ekman suction pump of an inner zone) and interactions between monsoon currents and terrain (including the local respond to the global scale) (Li, 2014), which results in seasonal sea level high or low in the coastal region of China. In the north coast of the Changjiang estuary, the residual water caused by Ekman is not obvious. The sea-side boundary shoreward accumulation or offshore loss caused by monsoon currents plays a key role. While in the South China Sea, significant seasonal sea level changes in the west coast are mainly dominated by surface Ekman transport and Ekman pumping due to the monsoon (Li, 2014; Liu et al., 2013).

In recent years, with the frequent occurrence of extreme weather and climate events, the anomalies of seasonal sea level increased, and they were more and more severe (Wang et al., 2014). “2012 Chinese Sea Level Bulletin” reported that the coastal sea level of the East China Sea (ECS) increased significantly in 2012 with the highest value in June and August since 1980. “2013 Chinese Sea Level Bulletin” reported that the coastal sea level of the ECS reached the highest value in May and October since 1980 (State Oceanic Administration, 2012, 2013).

Sea level anomalies are closely related to ENSO events. The

*Corresponding author, E-mail: hansz@ouc.edu.cn

primary driver of anomalous high or low water levels in the Pacific Ocean is the ENSO (Zervas, 2009). During normal periods, easterly equatorial winds maintain higher sea levels in the western Pacific. Occasionally, the winds weaken every 3–5 a, resulting in lower water levels in the western Pacific and higher water levels and ocean temperatures in the central and eastern equatorial Pacific. When the easterly equatorial winds are stronger than normal, La Niña happens (Zervas, 2009; Rong et al., 2007; Yamagata et al., 1985). During La Niña, the warmer SST in the western tropical Pacific around the Philippines induces stronger convection activities, which result in the western Pacific subtropical high northward migration. At the same time, SST in the northwest Pacific Ocean rises, and the Kuroshio Current strengthens, which favors the rise of sea level (Chen and Ma, 2013; Chen et al., 2012).

Xisha sea area is located in the South China Sea, which is a typical monsoon climate zone. It is also a key area to monitor the sea level rise. This paper analyzes the characteristics and causes of seasonal changes of sea level anomaly of Xisha sea area.

2 Data

The sea level data used in this paper are from Xisha hydrological observation station and satellite altimeter. The hydrological observation station is from National Marine Data and Information Service (NMDIS), China. The data is from January 1989 through December 2013, a total of 300 months. The sea level data has been supplemented and revised with the same zero reference (Wang et al., 2013). Satellite altimetry data (SSH) is a fusion of multiple satellite data (Jason-1/2, T/P, Envisat, GFO, ERS-1/2, GEOSAT), produced by French Space Research Centre, named Archiving, Validation and Interpretation of Satellite Oceanographic (AVISO). It is a monthly mean sea level anomaly (MSLA) data with a Mercator grid that the spatial resolution is $(1/3)^\circ \times (1/3)^\circ$. The MSLA data is from January 1993 through December 2013, a total of 252 months. Its area is $18^\circ\text{--}40^\circ\text{N}$, $110^\circ\text{--}130^\circ\text{E}$, covering China Paracel Islands, Zhongsha Islands and Nansha Islands. The data have been revised and quality controlled.

Wind field data used in this study is provided by the National Centers for Environmental Prediction (NCEP) / US National Center for Atmospheric Research (NCAR), the spatial resolution is $1^\circ \times 1^\circ$ (10 m wind), for the period 1981–2013.

Currents and SST data come from the reanalysis monthly mean data products (SODA data set) developed by University of Maryland (UMD) and Texas A & M University (TAMU), and the version of the data is the SODA-2.2.4 with $0.5^\circ \times 0.5^\circ$ resolution in the horizontal direction. In this article the currents and SST in 25 m layer are used.

All the elements in this paper use the average values during the years 1993–2011 as the multi-year average, and the monthly mean values during that period as the monthly multi-year average. The anomalies are the difference between mean values and the values of that period during 1975–1993.

3 The anomalies changes of sea level in the Xisha sea area

In this section, we analyzed the anomalous characteristic of Xisha surrounding sea area using the hydrological observation station and satellite altimeter data. In June 2010, the sea level in Xisha surrounding sea area decreased slightly, 6 cm lower than normal. In July of 2010, the sea level rose rapidly, nearly 20 cm higher than that of the same period in the history. In August of 2010, the sea level was 34 cm higher than that of the same period

in the history. The sea level had risen 43 cm from June to August, with the strength twice the annual variation range. Since September, the sea level began to fall, gradually closing to the normal in December (Fig. 1). The sea level in the Xisha sea area showed strong seasonal cycle. The sea level is the highest in July and August, while it is the lowest in January and February. The annual variation range is 21 cm.

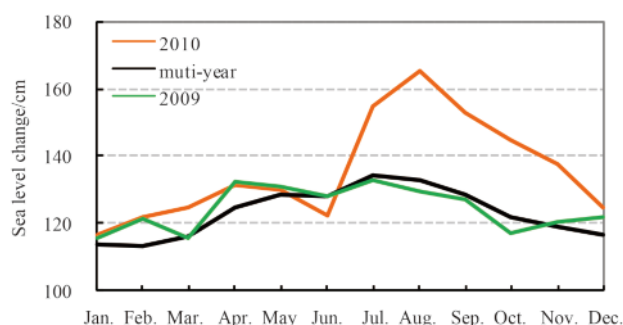


Fig. 1. Seasonal sea level change in the Xisha sea area.

The sea level high anomaly in the Xisha sea area for several months raised the average value throughout the year. Using the station observation and the satellite altimeter data separately calculated the trend of sea level in the Xisha sea area from 1993 to 2013 (Fig. 2). Figure 2 shows that the analysis results of stations and satellite data are similar, and the sea levels generally fluctuating rise with the rate of 5.5 mm/a and 5.9 mm/a respectively, much larger than that of the global (2.8 mm/a) and the Chinese offshore (3.7 mm/a). The sea levels were in high values in 1998, 2001, 2008, 2010 and 2013, which reached the highest in 2010 in the history, and the sea levels were lower during 1993–1997 and 2004–2006.

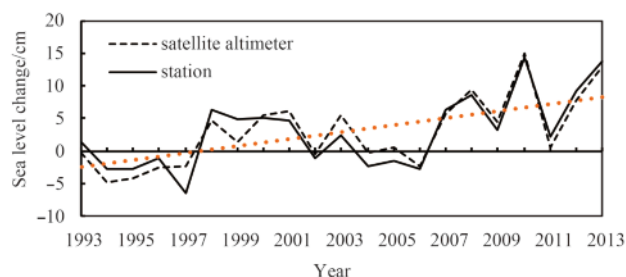


Fig. 2. Sea level changes around the Xisha sea area during 1993–2013.

In order to find out the scope of the anomalous high sea level in the Xisha sea area, we used satellite altimeter data to analyze the sea level anomalies in July and August 2010 and compare with those in July and August 2009 (Figs 3 and 4). As shown in Fig. 3, in July 2010, there are two obvious high value areas from eastern coastal region of Vietnam to the Xisha surrounding waters. The highest value appears in the eastern coastal waters of Vietnam with the anomaly of 45 cm, and the anomaly of Xisha surrounding waters reached 30 cm. In August 2010, the high-value area of sea level anomalies transfer to the Xisha surrounding waters with the sea level anomaly value of 45 cm. Sea level anomalous heights of the two months in the Xisha sea area are consistent with the results in Fig. 1.

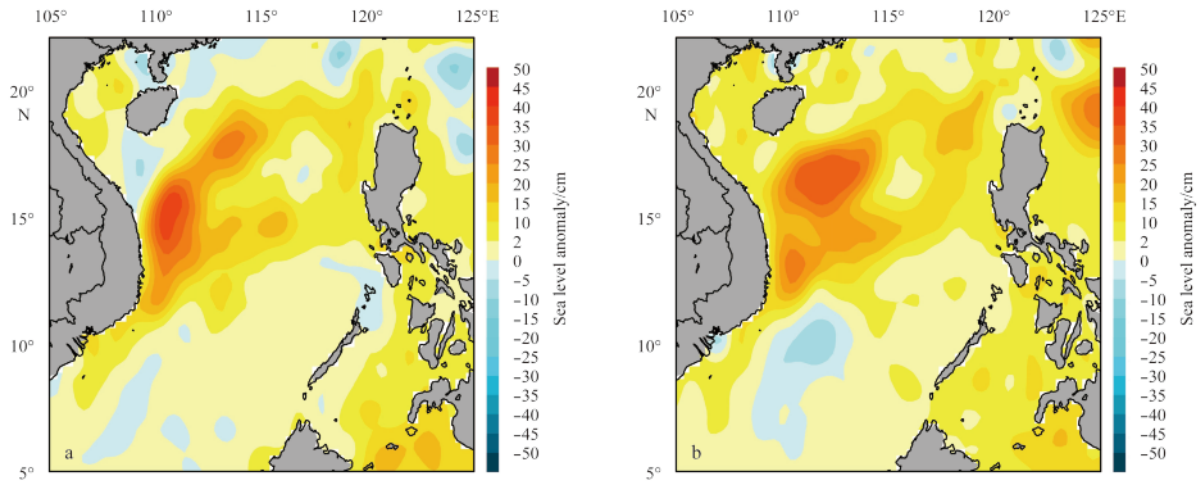


Fig. 3. Sea level anomaly fields in July (a) and August (b) 2010.

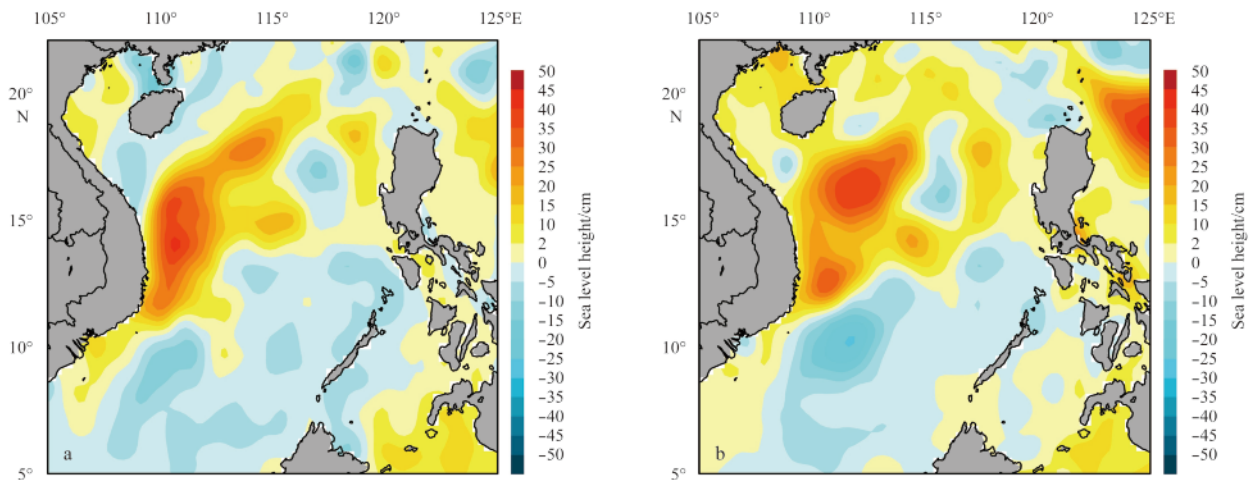


Fig. 4. Sea level heights in July (a) and August (b) 2010 compared with that of the same period of 2009.

Figure 4 shows the difference between sea level of the study area in July and August 2010 and that of July and August 2009. The high value region of the sea level is extremely close to the region in Fig. 3. The highest value appears in the Xisha surrounding waters with 45 cm in August, and the sea level in the west of Nansha is lower in comparison with 2009. Especially in August, in the center of 16.50°N, 112°E and 10°N, 112°E sea level difference reached 70–80 cm.

4 The relationship between sea level of Xisha and ENSO

4.1 Spatial and temporal distribution of sea-level changes

In order to further analyze the characteristics of sea level change in Xisha surrounding areas and the relationship with ENSO, the Empirical Orthogonal Function (EOF) analysis (Chen and Ma, 1991) was performed on the SSH anomaly field (5°–20°N, 108°–120°E) over 21 years. Results are presented in Figs 5 and 7. The first two modes account for 77.5% and 8% of the total variance, respectively. The SSH EOF spatial pattern and principle component time series of the first mode (PC1) shows the rising sea levels in the north region and the falling sea levels in the south-west region in Sansha area. The sea level rises significantly in Paracel Islands (14°–17°N, 110°–113°E) and Zhongsha Islands

(14°–17°N, 116°–120°E), while it decreased in the western sea area of the Nansha Islands (5°–10°N, 108°–113°E).

In order to further investigate the interannual variability of sea levels in this region, the Morlet wavelet transform analysis (Farge, 1992; Lau and Weng, 1995) was carried out on SSH PC1, and the result is shown in Fig. 6. As can be seen, sea level has notable periods of 2–3 a, 5 a and quasi 9 a in the region. The quasi 9 a periodic oscillation is the most significant, which is the period of tidal astronomical tide, reflecting the variation of moon declination, also known as the intersection tide (Fang et al., 1986; Yu, 2004). Its amplitude was the largest in this area. Since the data sequence is only 21 years, therefore it cannot reflect the significant decadal change period.

The explained variance of the second mode is 8%, which exhibits the characteristics of interannual variations of the sea level (Fig. 7). The spatial distribution and temporal changes show that, the sea level in Paracel Islands surrounding sea area (11°–17°N, 110°–114°E) exist significant interannual change, which is higher in 1998 and 2010 over the past 21 years. The anomalous high amplitude is the strongest in 2010. Combined with Fig. 1 of third chapter, the sea level is 19–34 cm higher than the same period of the multi-year mean in the region in July to November 2010 and the highest in August.

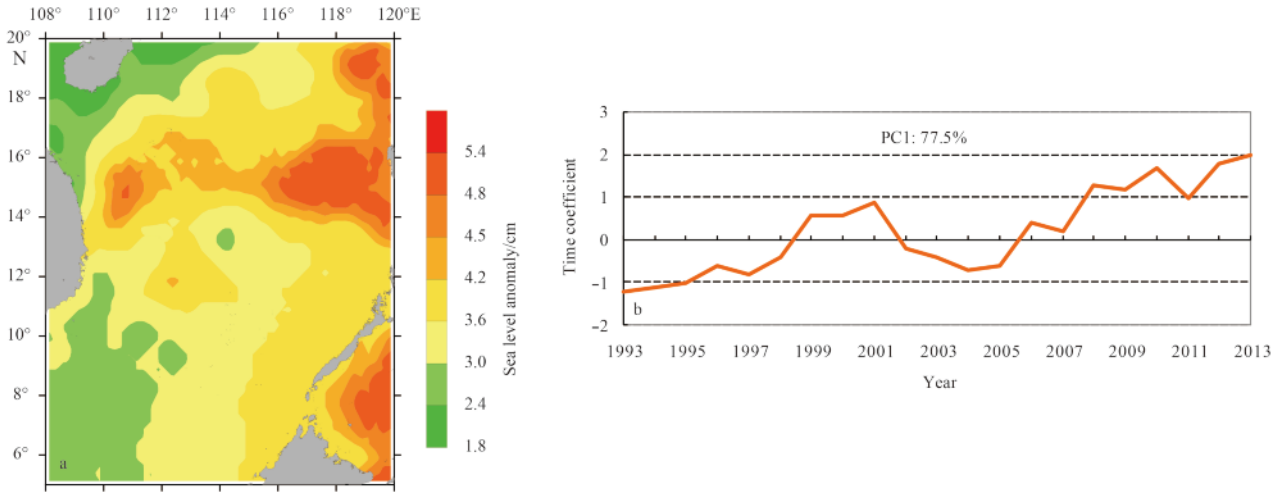


Fig. 5. The space distribution (a) and corresponding time coefficient (b) of first EOF mode for sea level anomaly.

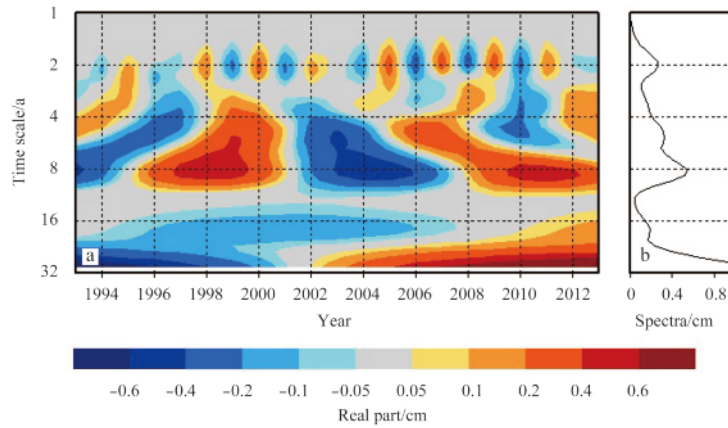


Fig. 6. Wavelet transform analysis on the time coefficient of first EOF mode for sea level anomaly. a. The real part of wavelet spectrum and b. the right are wavelet spectrum.

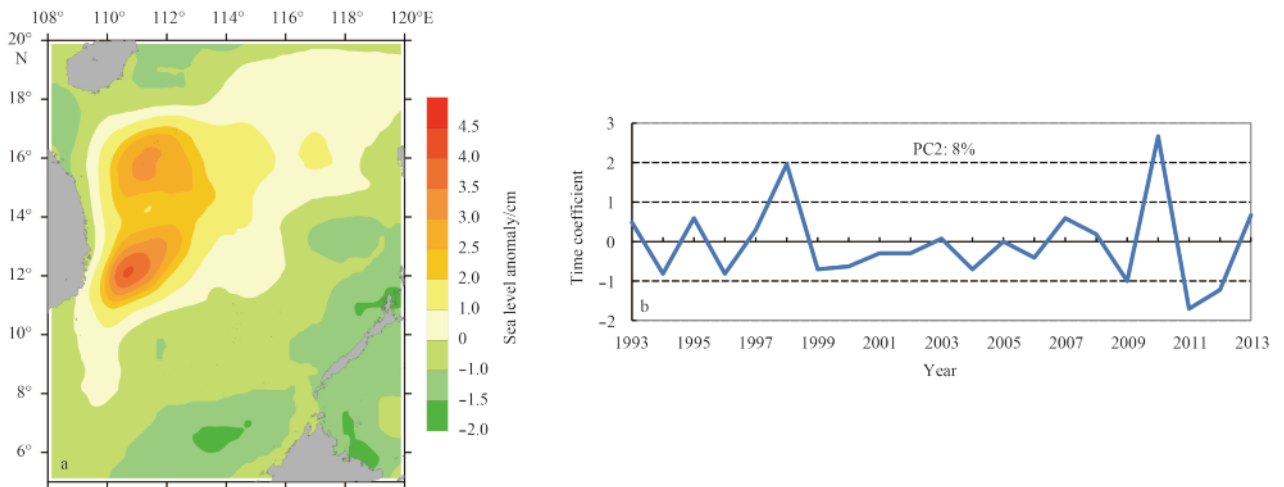


Fig. 7. The space distribution (a) and corresponding time coefficient (b) of second EOF mode for sea level anomaly.

In order to further investigate the interannual variability of sea levels in this region, the Morlet wavelet transform analysis was carried out on SSH EOF principle component time series of the second mode (PC2), and the result is shown in Fig. 8. Com-

pared with spatial and temporal variation of the second mode, we can see that sea level has notable periods of 2–3 a, 4 a, 7 a and quasi 9 a. The 2–3 a oscillation is the most significant, which is weather period. Under the effect of the monsoon, the interaction

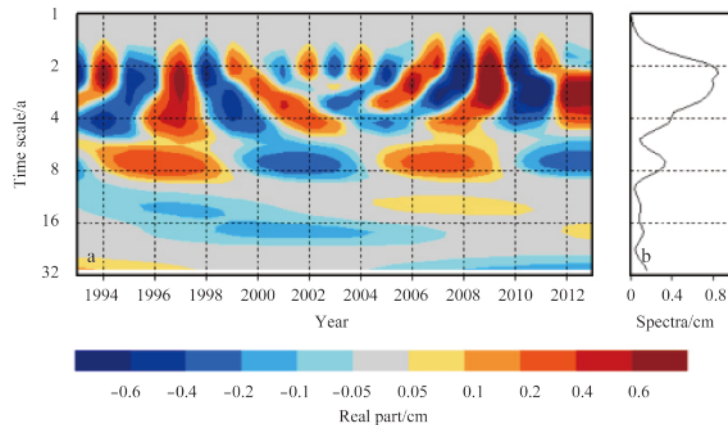


Fig. 8. Wavelet transform analysis on the time coefficient of second EOF mode for sea level anomaly. a. The real part of wavelet spectrum and b. the right are wavelet spectrum.

of the quasi 2 a oscillation of tropical western Pacific and ENSO can make ENSO have a quasi 2 a or quasi 7 a period (Liu et al., 2006). The anomalous high or low sea level in the region is close to monsoon and ENSO events.

4.2 The relationship between sea level anomalies and ENSO

Figure 7 shows that the sea levels in the study region (11° – 17° N, 110° – 114° E) over the past 21 years showed strong interannual anomalies. The sea levels were anomalous high from June through November in 1998, and they were anomalous high from July to November in 2010. As can be seen, this time was in the La Niña period. In 1998/1999 and 2010/2011, the La Niña events occur two times immediately after the El Niño events

(1997/1998 and 2009/2010). During the El Niño events, the sea levels were lower, and then the occurrence of La Niña is accompanied with significantly higher of the sea level (Table 1). Tidal harmonic analysis to Xisha sea area found that the amplitudes and the phases of the solar annual constituent Sa are great different. In El Niño years, the annual amplitudes decreased, and the phases advanced. Such as in 1997 and 2009, amplitudes of Sa were respectively 11.9 cm and 7.3 cm, and the phases were respectively 99.4° and 95.1° . However, in La Niña years, amplitudes were significantly higher, and the phases significantly lagged. Such as in 1998 and 2010, amplitudes of Sa were respectively 18.4 cm and 16.6 cm, and the phases were respectively 150.3° and 153.1° .

Table 1. Monthly sea level anomalies (Unit: cm), amplitude and phases of Sa in Xisha sea area during ENSO

Year	Jan.	Feb.	Mar.	Apr.	May	Jun.	Jul.	Aug.	Sep.	Oct.	Nov.	Dec.	Amplitude/cm	Phase/($^{\circ}$)
1997	-8.8	-6.2	-6.1	-4.4	-4.4	-5.6	-1.0	-5.6	-13.4	-16.5	-12.2	-4.3	12.9	99.4
1998	2.3	2.6	0.7	-10.6	0.2	8.0	7.1	8.5	18.8	12.6	14.7	1.5	16.6	150.3
1999	6.1	5.2	11.4	7.5	-8.1	3.5	10.6	-0.3	0.1	4.8	1.2	6.7	8.29	112.2
2009	3.1	5.2	11.4	7.5	-8.1	3.5	10.6	-0.3	0.1	4.8	1.2	6.7	7.3	95.1
2010	4.3	10.2	10.1	8.3	2.6	-6.3	22.2	33.6	25.7	23.4	19.2	9.3	18.4	153.1
2011	11.6	13.3	6.5	4.3	6.7	2.9	-5.0	-7.3	-3.8	-9.0	-5.1	0.9	8.2	60.8

In order to further analyze the relationship between the sea level variation surrounding Xisha sea area and ENSO, the averaged seasonal cycle are removed from the monthly sea level (MSL) series, the residual series represents the interannual MSL variability. Then, the sea level residual series and different Niño indices (Niño 4 and Niño 3.4) are analyzed. The result shows that there is a significant negative correlation between sea level and Niño indices (Niño 4 indice and Niño 3.4 indice), and the lag correlation coefficients with Niño 4 indice and Niño 3.4 indice for 2 months and 3 months are -0.46 and -0.45, respectively. All the statistical significance tests for partial correlations are performed using the t-test. The degrees of freedom used for such a test are 250 for a time series of 252 months. The correlation coefficients at significance levels 95% and 99% are 0.13 and 0.18, respectively (Fig. 9).

The regional sea level anomalies were affected by hydrological and meteorological factors besides ENSO events. In the next section, we focus on the changes of the wind field, flow field and sea surface temperature during sea level season anomalies period (July to August) surrounding Xisha sea area in 2010.

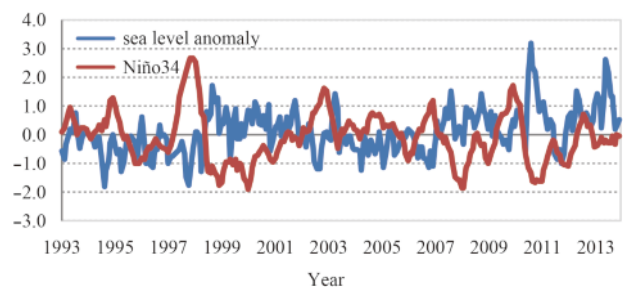


Fig. 9. The changes of monthly sea level anomaly and Niño 34 in Xisha sea area (Unit: cm).

5 Possible causes of sea level anomalies

5.1 Wind and flow

Compared with the same period of the normal year (Fig. 10), the wind anomaly sustains strong in the south of Sanaha, and in Xisha area it is apparent northeast wind field anomaly with wind speed anomaly value of 4 m/s in July 2010. The wind field shift

northward and southward respectively in the eastern sea area of Vietnam, forming a clockwise vortex in the Paracel Islands surrounding sea area in the north of 15°N. In August, wind anomaly weakened and Xisha sea area was substantially northeast anomaly wind, but in the Paracel Islands surrounding sea area, it turned to the east anomaly wind. Since June 2010, La Niña happens (2010/2011), which is the strongest in the history. ENSO has

a significant impact on the South China Sea monsoon, and the local air sea system is an important part of ENSO (Webster and Yang, 1992; Huang et al., 2003; Li, 2014). ENSO affects the South China Sea (SCS) sea level by the north wind anomaly and the North Pacific Ocean Circulation (Kuroshio Current) (Rong et al., 2007). In the South China Sea, the correlation coefficient between radial wind stress and non steric sea level height is 0.7 (Ding et

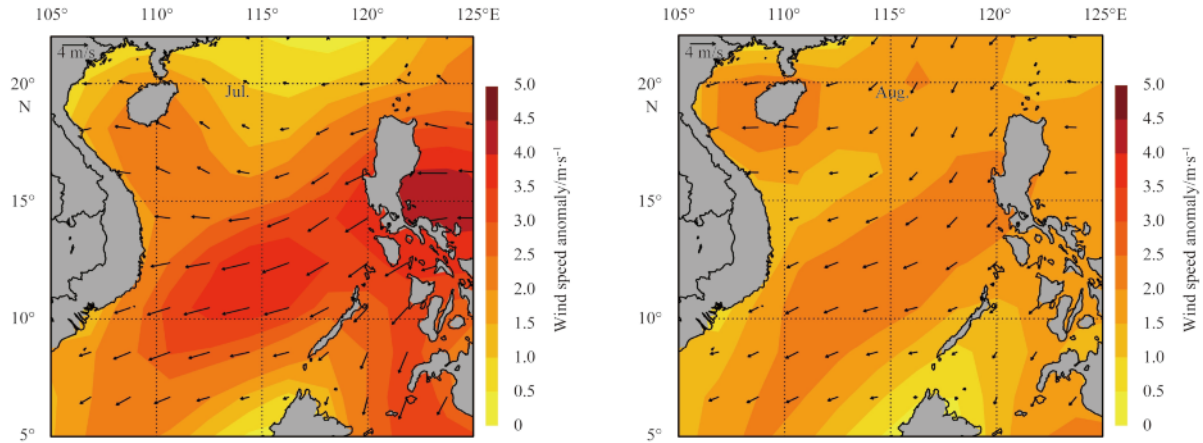


Fig. 10. Wind speed anomaly fields in July and August 2010.

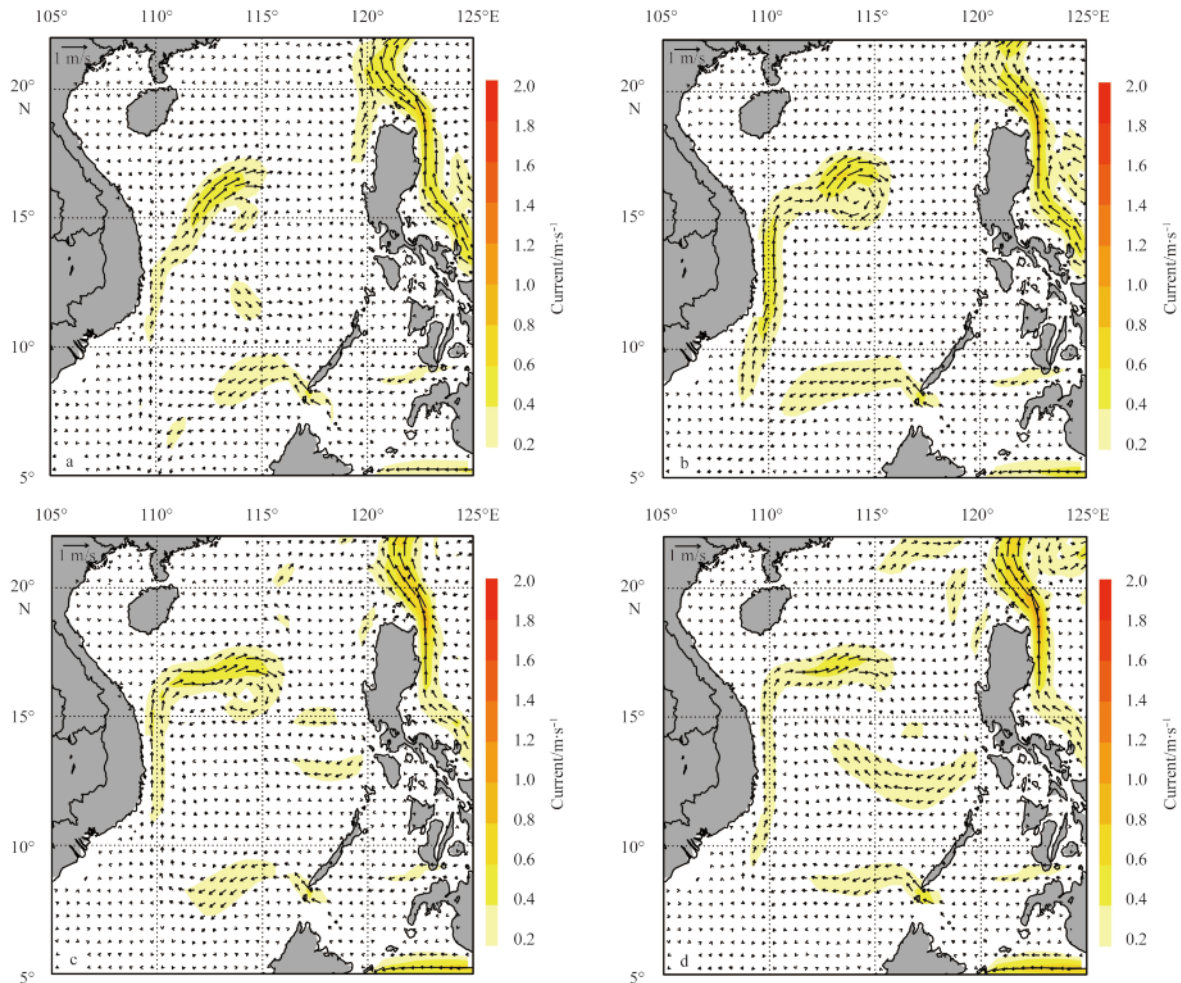


Fig. 11. The 25 m layer flow field changes in Xisha sea area from June to September 2010. a. June, b. July, c. August, and d. September.

al., 2007). The local wind field effect on marine vortex is significant (Chen and Wang, 2014).

Circulation in the South China Sea is relatively independent, and the upper ocean circulation is driven mainly by the monsoon. The formation and maintenance of small scale circulation and vortex can be considered as the combined action of wind, submarine topography, the shape of the coastline and the inertia effect (Xie et al., 2003).

The flow field changes of Sansha sea area from June to September 2010 are shown in Fig. 11. In June, there was a northward flow in the east coast of Vietnam. It turned to northeast in the Paracel Islands surrounding sea area with flow velocity close to the velocity of the Kuroshio near the Luzon Strait of 0.8 m/s and formed a small vortex in the southern region. In July, the north flow field became larger and a strong vortex was formed in the Paracel Islands surrounding sea area with the rate of 1.0 m/s, and maintained until August. In September, the north flow field weakened, and the vortex gradually disappeared. Compare Fig. 1, Fig. 3 and Fig. 4 with each other, we can see that the time and region of vortex formation and disappearance match with that of sea-level abnormal changes from July to September 2010.

There is a certain relationship between the South China Sea vortex and the ENSO events (Chu et al., 2014). The life cycle of

most eddies is within 180 days, with radius of 100 km to 250 km, and its radial variation is consistent with the radial change of baroclinic Rossby wave. The South China Sea vortex occurs mainly in the east of Vietnam to the southwest of Taiwan, and its contribution to the sea level change as high as 80% (Lin et al., 2007).

5.2 SST

In summer and autumn, there is a cold vortex on the coast of Vietnam. The Vietnam cold eddy is related to the seasonal upwelling, corresponding to the cyclonic circulation of small scale and positive wind stress curl. In addition, there is a stronger warm eddy in the south of cold eddy, which corresponds to an anticyclonic circulation (Xie et al., 2003).

The 25 m layer temperature field distributions of Sansha and surrounding sea area in July and August 2010 and in July and August 2009 are shown in Figs 12 and 13, respectively. In July and August 2009, a cold eddy entrenched in the eastern waters of Vietnam with the SST up to 26–27°C, which was 1–2°C lower than that of the surrounding sea area. However, in July and August 2010, the SST in this region increased significantly, up to 28–30°C, which was 2–3°C higher than that of the same period in 2009. In the South China Sea, the steric sea level changes caused by sea

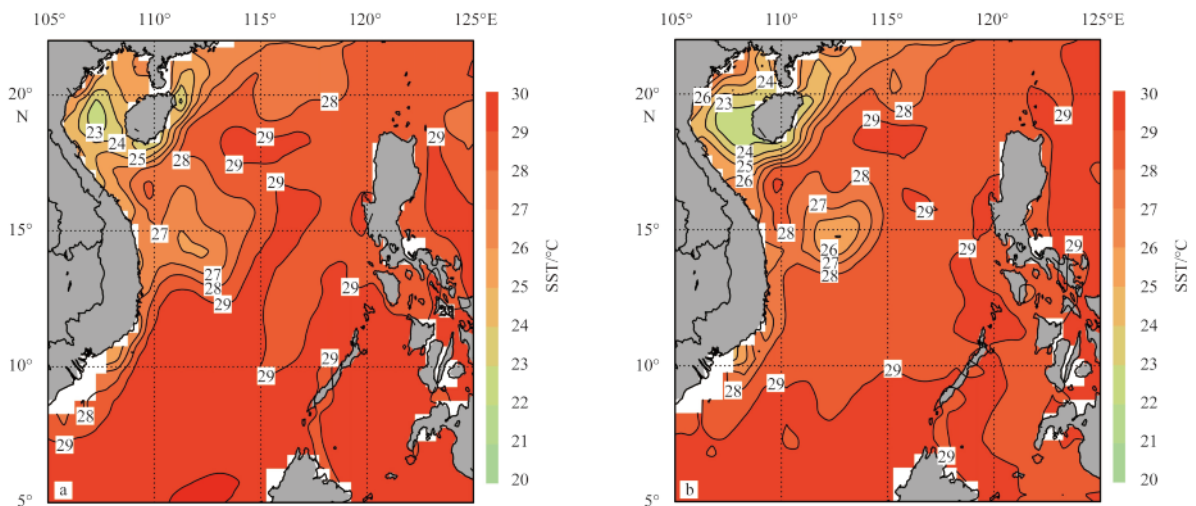


Fig. 12. The 25 m layer SST distributions in Xisha surrounding sea area in July (a) and August (b) 2009.

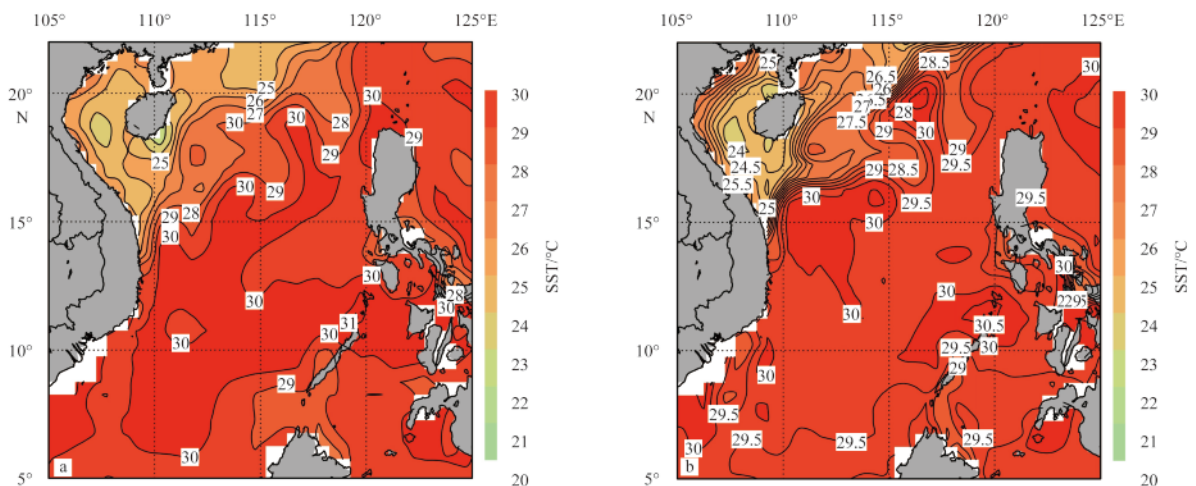


Fig. 13. The 25 m layer SST distributions in Xisha surrounding sea area in July (a) and August (b) 2010.

temperature lead to the change of sea level height, and its contribution to roughly 89.4% (Ding et al., 2007; Zuo et al., 2009).

Through a comparative analysis we found that in July and August 2010, the area of sea level high anomaly is consistent with that of warm sea surface temperature and the position of the vortex flow field. Xu et al. (2008) put forward that at small spatial scales, there was a positive correlation between SST and surface wind speed, which reflects the forcing of ocean to atmosphere.

6 Conclusions

In this paper, in connection with the characteristics of the sea level variation in the Xisha sea area, the factors that may cause sea level anomalous high were analyzed in detail. The analysis results show that:

(1) Since 1993, the sea level in the Xisha sea area was obviously higher than normal in 1998, 2001, 2008, 2010 and 2013. Especially, the sea level was higher in 1998 and 2010, and the sea level in 2010 was 13.2 cm higher than the multi-year mean, which is the highest in the history.

(2) Sea level in the Xisha sea area rises significantly with increased rate of 5.5 mm/a since 1993, much higher than the rate of China's coastal and global sea level rise over the same period. The sea level of the area has multiple significant oscillation periods of 9 a, 2–3 a and 4–7 a. It indicates that the sea level of the area is not only affected by the tidal force of the celestial bodies, but also closely related to the tropical western Pacific monsoon in the area of quasi-periodic oscillation 2 a and ENSO events.

(3) There is a significant negative correlation between sea level in the Xisha sea area and ENSO events. The sea level anomalous high occurred during the developing stage of La Niña. It also shows negative correlation with Niño 4 indice and Niño 3.4 indice prominently, and the lag correlation coefficients for 2 months and 3 months are -0.46 and -0.45, respectively.

(4) In 2010, during the period of sea level anomaly, in the early La Niña events, the anomalous wind field was cyclonic circulation. The current in 25 m layer form a strong clockwise vortex in the area, and the current rate close to the speed of the Kuroshio near the Luzon Strait. In normal years, there is a "cool eddy", while in 2010, from July to August, the SST in the area was 2–3°C higher than that of the same period in the history.

References

- Chen Shangji, Ma Jirui. 1991. *Marine Data Processing Analysis Methods and Their Applications* (in Chinese). Beijing: China Ocean Press, 312–318
- Chen Changlin, Wang Guihua. 2014. Interannual variability of the eastward current in the western South China Sea associated with the summer Asian monsoon. *Journal of Geophysical Research: Oceans*, 119(9): 5745–5754, doi: 10.1002/2014JC010309
- Chen Yongli, Zhao Yongping, Feng Junqiao, et al. 2012. ENSO cycle and climate anomaly in China. *Chinese Journal of Oceanology and Limnology*, 30(6): 985–1000
- Chen Yongli, Zhao Yongping, Wang Fan. 2013. ENSO and the Marine Environment and Climate Anomalies of China (in Chinese). Beijing: Science Press, 23–25
- Chu Xiaoqing, Xue Huijie, Qi Yiquan, et al. 2014. An exceptional anticyclonic eddy in the South China Sea in 2010. *Journal of Geophysical Research: Oceans*, 119(2): 881–897, doi: 10.1002/2013JC009314
- Ding Rongrong, Zuo Juncheng, Du ling, et al. 2007. Sea level change in the South China Sea and its relations to the steric height variation and wind. *Periodical of Ocean University of China* (in Chinese), 37(Sup II): 23–30
- Fang Guohong, Zheng Wenzhen, Chen Zongyong, et al. 1986. *Analysis and Forecast of Tidal and Current* (in Chinese). Beijing: China Ocean Press, 268–281
- Farge M. 1992. Wavelet transforms and their applications to turbulence. *Annual Review of Fluid Mechanics*, 24(1): 395–458
- Huang Ronghui, Chen Wen, Ding Yihui, et al. 2003. Studies on the monsoon dynamics and the interaction between monsoon and ENSO cycle. *Chinese Journal of Atmospheric Sciences* (in Chinese), 27(4): 484–502
- Intergovernmental Panel on Climate Change (IPCC). 2013. *Climate Change 2013: The Physical Science Basis. Contribution of Working Group I to the Fifth Assessment Report of the intergovernmental Panel on Climate Change*. Cambridge: Cambridge University Press
- Lau K M, Weng Hengyi. 1995. Climate signal detection using wavelet transform: how to make a time series sing. *Bulletin of the American Meteorological Society*, 76(12): 2391–2402
- Li Li. 2014. The meridional sea level oscillation of the China seas and the Gulf of Thailand. *Haiyang Xuebao* (in Chinese), 36(9): 7–17
- Lin Pengfei, Wang Fan, Chen Yongli, et al. 2007. Temporal and spatial variation characteristics on eddies in the South China Sea I. Statistical analyses. *Haiyang Xuebao* (in Chinese), 29(3): 14–22
- Liu Qinyu, Liu Zhengyu, Pan Aijun. 2006. Conceptual model about the interaction between El Niño/Southern Oscillation and Quasi-Biennial Oscillation in far west equatorial Pacific. *Science in China Series D: Earth Science*, 49(8): 889–896
- Liu Qinyu, Xie Shangping, Zheng Xiaotong. 2013. *Tropical Ocean-Atmosphere Interaction* (in Chinese). Beijing: Higher Education Press, 9
- Rong Zengrui, Liu Yuguang, Zong Haibo, et al. 2007. Interannual sea level variability in the South China Sea and its response to ENSO. *Global and Planetary Change*, 55(4): 257–272
- State Oceanic Administration. 2012. 2011 Bulletin of the sea level of China (in Chinese). Beijing: State Oceanic Administration
- State Oceanic Administration. 2013. 2012 Bulletin of the sea level of China (in Chinese). Beijing: State Oceanic Administration
- Wang Hui, Fan Wenjing, Li Yan, et al. 2012. Analysis on sea level anomaly in the coastal area of Bohai Sea and Yellow Sea in February. *Marine Science Bulletin* (in Chinese), 31(3): 255–261
- Wang Hui, Liu Kexiu, Fan Wenjing, et al. 2013. Data uniformity revision and variations of the sea level of the western Bohai Sea. *Marine Science Bulletin* (in Chinese), 32(3): 256–264
- Wang Hui, Liu Kexiu, Fan Wenjing, et al. 2014. Analysis on the sea level anomaly high of 2012 in China coastal area. *Haiyang Xuebao* (in Chinese), 36(5): 8–17
- Webster P J, Yang S. 1992. Monsoon and ENSO: selectively interactive systems. *Quarterly Journal of the Royal Meteorological Society*, 118(507): 877–926
- Xie Shangping, Xie Qiang, Wang Dongxiao, et al. 2003. Summer upwelling in the South China Sea and its role in regional climate variations. *Journal of Geophysical Research: Oceans*, 108(C8): doi: 10.1029/2003JC001867
- Xu Haiming, Wang Linwei, He Jinhai. 2008. Observed oceanic feedback to the atmosphere over the kuroshio Extension during spring time and its possible mechanism. *Chinese Science Bulletin*, 53(12): 1905–1912
- Yamagata T, Shibao Y, Umatani S I. 1985. Interannual variability of the Kuroshio Extension and its relation to the Southern Oscillation/El Niño. *Journal of the Oceanographical Society of Japan*, 41(4): 274–281
- Yu Yifa. 2004. Advance of the researches on the variations of mean-sea-level (MSL) in the coastal waters of China. *Periodical of Ocean University of China* (in Chinese), 34(5): 713–719
- Zervas C E. 2009. *Sea level variations of the United States, 1854–2006*. Silver Spring, MD: US Department of Commerce, National Oceanic and Atmospheric Administration
- Zuo Juncheng, Zhang Jianli, Du Ling, et al. 2009. Global sea level change and thermal contribution. *Journal of Ocean University of China*, 8(1): 1–8